Applied Catalysis B: Environmental 285 (2021) 119819

Contents lists available at ScienceDirect

Applied Catalysis B: Environmental

journal homepage: www.elsevier.com/locate/apcatb

Elucidating the role of ethanol in aqueous phase hydrodechlorination of trichloroethylene over Pd catalysts supported on swellable organically modified silica (SOMS)

Saurabh Ailawar [a], Anagha Hunoor [a], Yehia Khalifa [b], Jeffrey T. Miller [c], Paul L. Edmiston [d], Umit S. Ozkan [a,*]

[a] William G. Lowrie Department of Chemical and Biomolecular Engineering, The Ohio State University, 151 W. Woodruff Avenue, Columbus, OH, 43210, USA
[b] Department of Chemistry and Biochemistry, The Ohio State University, 151 W. Woodruff Avenue, Columbus, OH, 43210, USA
[c] Davidson School of Chemical Engineering, Purdue University, 480 Stadium Mall Drive, West Lafayette, IN, 47907-2100, USA
[d] Department of Chemistry, The College of Wooster, 943 College Mall, Wooster, OH, 44691, USA

ARTICLE INFO

Keywords:
Swellable organically modified silica (SOMS)
Palladium
Hydrodechlorination
Catalyst deactivation
Trichloroethylene
Near-ambient pressure X-ray photoelectron spectroscopy (NAP-XPS)
Hydrophobicity

ABSTRACT

In this study, effect of ethanol on the performance of Pd supported on swellable organically modified silica (SOMS) for hydrodechlorination (HDC) of trichloroethylene (TCE) is investigated. SOMS is a hydrophobic material that swells to 3–4 times its original volume when contacted with organic solvents. Catalytic HDC of TCE suffers from inhibition due to HCl which is worsened by the slow removal of HCl from the hydrophobic pores of SOMS. Addition of ethanol resulted in swelling of SOMS matrix causing expansion of pores, thereby facilitating the removal of HCl. The inhibitory effect of HCl was alleviated by ethanol, without altering the HDC reaction pathway. Characterization using near-ambient pressure X-ray photoelectron spectroscopy and extended X-ray absorption fine structure showed the effect of ethanol on swellability and HCl removal, respectively. Lastly, a mechanism has been proposed for the uninhibited reaction, which exhibited first order kinetics with respect to TCE.

1. Introduction

Heterogeneous catalysis research has primarily focused on the use of inanimate materials as catalyst scaffolds for small active metal particles. Animated materials possessing textural properties that are responsive to the environmental conditions is an emerging class of materials in catalysis [1]. Swellable organically modified silica (SOMS) is one such animated material which responds to the presence of organic solvents through expansion up to four times its original volume [2].

SOMS is a type of hybrid organic-inorganic materials, which are commonly referred to as bridged polysilsesquioxanes [2–4]. The precursors used for these materials typically contain two or more trifunctional silyl groups such as -$Si(OCH_3)_3$ (trimethoxysilyl) or - $Si(OC_2H_5)_3$ (triethoxysilyl), which are covalently bonded to an organic functional group (also known as spacers) such as aryl, alkyl, alkenyl groups etc [5–8]. The covalent bonds between the Si atoms and the terminal C atoms of the spacer are non-hydrolyzable, allowing polymerization to occur only at the alkoxy groups attached to the trifunctional Si atoms [6, 8]. SOMS is synthesized using base-catalyzed sol-gel technique with bis (trimethoxysilylethyl)benzene (BTEB) as the precursor. It is hydrophobic, mesoporous and possesses high surface area as well as high sorption capacity [2–4,9].

Although, bridged polysilsesquioxanes are frequently studied, their 'swellable' counterparts are rarely encountered. During drying of the SOMS gel, flexibility of the ethyl bonds between the aryl and the silyl groups of BTEB aids in the self-assembly of aromatic rings in the structure resulting in π-π stacking. Interestingly, the elasticity of SOMS allows potential energy to be stored in the matrix in its shrunken form which is released upon solvent induced swelling, generating force [4]. It has been proposed that swelling is induced by organic solvents disrupting the non-covalent interactions (van deer Waals, π-π stacking) between collapsed interacting pore walls, causing matrix relaxation and rapid expansion of the material to ~2−4x in volume. Derivatization of the surface silanol groups with non-condensable -$Si(CH_3)_3$ groups is necessary to obtain the necessary flexibility in the organosilica matrix by preventing Si-O-Si crosslinking when SOMS gel dries. Swelling is

* Corresponding author.
E-mail address: ozkan.1@osu.edu (U.S. Ozkan).

https://doi.org/10.1016/j.apcatb.2020.119819
Received 26 September 2020; Received in revised form 2 December 2020; Accepted 5 December 2020
Available online 24 December 2020

regarded as a mechanical phenomenon instead of a chemical process [2,4,10,11]. As the matrix expands, the pore size increases accommodating the solvent molecules that are used to trigger swelling.

Swellable materials have applications in various fields such as chemical and optical sensing, membrane-based gas separation, drug-delivery systems, environmental remediation and catalysis [12–17]. Swellable materials studied in catalysis include polyionic liquids (PILs), polysiloxanes and cross-linked functional polymers (CFPs) among which CFPs have been largely studied [1,18–20]. Homo-polymerization or co-polymerization of vinyl monomers such as styrene, divinylbenzene (DVB) etc., forms cross-linked polymers generally known as CFPs [1]. These polymers have been used as catalyst scaffolds for reduced nano-clusters of metals such as Pd, Au, Cu, Pt etc., for liquid phase hydrogenation and oxidation reactions [1,21,22]. These swellable materials are functional under fully swollen conditions in the liquid phase where the solvation-ability of a solvent determines the extent of swelling [1]. To that end, polarity of the solvent and the hydrophobic/hydrophilic nature of the CFPs is largely found to affect the solvation-ability [23,24]. Upon solvation of the polymeric chain, these materials behave as a 'viscous pseudosolution or suspension' rather than as solid material providing accessibility to internal surface area. Extensive characterization of these materials aided in quantitatively studying the relation between morphology of the swollen CFPs and mobility of different solvents inside them [25–27]. These materials are known to suffer from low mechanical and thermal stability. For CFPs, the range for temperature of thermal decomposition under inert atmosphere is (200−300 °C) [1]. Recently, thermal decomposition performed during thermogravimetric analysis revealed that SOMS possessed a higher thermal stability (450 °C) as compared to CFPs [28]. Furthermore, in-situ characterization of metal particles incorporated in CFPs, under swollen conditions, is rarely performed.

Pd impregnated on SOMS was recently shown to be active for hydrodechlorination (HDC) of trichloroethylene (TCE) performed in both, gas and liquid phase environments, with commercial Pd/Al_2O_3 catalyst used for comparison [29–33]. TCE is one of the most toxic volatile organic contaminants found in groundwater with very low solubility (1200 ppm at room temperature) [34,35]. The maximum allowable concentration limit of TCE in drinking water is 5 ppb and it is listed as a priority contaminant by US. E.P.A. [36]. Although, catalytic HDC of TCE is found to be more effective than other remediation techniques such as, adsorption on activated carbon, oxidation and microbial degradation, it suffers from slow kinetics due to low concentration of TCE available in groundwater, deactivation due to dissolved anions and inhibition due to HCl produced during HDC [37,38].

Inhibition due to HCl has been the subject of many HDC studies aimed at designing heterogeneous catalysts with enhanced deactivation resistance. Some studies have employed Cl scavenging agents such as NaOH and KOH [39–41]. The use of these strong bases is often deleterious, as the excess hydroxyl ions tend to alter the surface charge of the support thereby altering the reaction rate [39,40]. Bimetallic configurations such as, Pd-Au change the electronic structure of Pd and increase the resistance to chloride deactivation [42,43]. Bimetallic nanoparticles formed with Ni and Fe, stabilized using surfactants have also been reported to exhibit good catalytic activity for HDC of TCE [44]. Several other studies make use of hydrophobic zeolite materials as supports for Pd as well as use of polymeric coating on Pd/Al_2O_3 which was later found to be degraded in the presence of HCl [45–48].

Our recent work demonstrated the deactivation resistance of Pd/SOMS towards chlorine and sulfur containing species [31,33]. The swelling ability of SOMS is crucial for depositing active Pd particles deep inside the pores, as verified by the inaccessibility for gas phase CO molecules [32]. It was also reported that the pore-size distribution of SOMS shifted from 5.4 nm to 3.9 nm after impregnation of Pd suggesting the deposition of Pd particles on the pore-walls [32]. However, the BET surface area of bare and Pd impregnated SOMS was almost the same [32]. Furthermore, bulk characterization such as X-ray absorption spectroscopy (XAS) revealed the absence of Pd-Cl and Pd-S interactions, suggesting better protection from liquid phase chloride species and gas-phase H_2S. The hydrophobicity of SOMS along with deeper impregnation of Pd particles inside the pores was considered responsible for enhanced deactivation resistance [31,33]. Performing reactions in presence of swelling agents such as ethanol, afforded swelling of SOMS, leading to better TCE conversion. It was then suggested that, ethanol may allow better accessibility to Pd species by swelling SOMS as well as facilitate the removal of HCl formed in the reaction [32]. In the present contribution, the role of ethanol during HDC of TCE on Pd/SOMS is elucidated while discussing the reaction kinetics. Furthermore, the effect of concentration of ethanol on the extent of swelling is evaluated using characterization and activity experiments. From the observed kinetics and mass-transfer results, a mechanism is also proposed.

2. Experimental section

2.1. Catalyst synthesis

Synthesis of SOMS was previously reported by Edmiston and co-workers [2,4]. Briefly, SOMS is synthesized using sol-gel method with bis-(trimethoxysilylethyl)benzene (BTEB) as the precursor, followed by addition of water (at a fixed mole ratio with BTEB) and tetrabutylammonium fluoride as the catalyst. After gelation and ageing, the material is washed with acetonitrile followed by derivatization of the surface silanol groups with hexamethyldisilazane (HMDS). The gel is then dried at room temperature followed by grinding in a ball mill at 200 rpm. The ground particles were sieved to obtain a particle size of <74 μm. For studies investigating the mass transfer limitations, SOMS particles ground to a size of 100−150 μm were obtained.

Pd/SOMS with a nominal metal loading of 1% was synthesized using incipient wetness impregnation (IWI) technique wherein, a solution with desired concentration of Pd(II) acetate (Sigma-Aldrich, 99.9 %) in acetone was added dropwise to a thin layer of ground SOMS particles. Visual swelling of SOMS particles was noted upon addition of the precursor solution. Intermittent drying of the support was carried out to remove excess acetone, at room temperature. After the entire solution was taken up by the support, it was dried overnight at room temperature. This catalyst was called unreduced Pd/SOMS in this study. For reduction, a known quantity of $NaBH_4$ was dissolved in 95% (v/v) ethanol-water solution. The quantity of $NaBH_4$ was decided to be in excess to ensure complete reduction of Pd acetate. This solution was slowly added to the unreduced Pd/SOMS and a visual color change from pale orange to black was observed. Post reduction, the catalyst was filtered and washed several times with ethanol to get rid of residual impurities. The catalyst was dried at 60 °C, overnight prior to use. 1% Pd/Al_2O_3 (commercial catalyst) was obtained from Sigma-Aldrich and reduced under H_2 for 3 h at 350 °C, prior to use.

2.2. Activity testing

Batch reactions were performed at 30 °C and 50 bar, using a 300 mL 4560 mini-benchtop stirred reactor from Parr Instruments Company. The reactor was equipped with 4848-controller for temperature and stirring speed with a PID program. 200 mL feed solution consisting of known concentration of TCE and tetrahydrofuran (THF) dissolved in water was added to the reactor vessel. THF was used as an internal standard. Once the reactor was sealed, the solution was bubbled with pure He in order to remove gaseous impurities present in the head-space as well as dissolved in the solution. The reactor speed was set to 2000 rpm and the temperature was stabilized at 30 °C. The reactor was pressurized in two steps. Initially, 45 bar of pure H_2 was introduced into the reactor and a sample was drawn out from the liquid phase to obtain the initial concentration of TCE (time = zero sample). As soon as the initial sample was collected, the total pressure of the reactor was raised to 50 bar by introducing H_2 through a customized catalyst addition

device (CAD) and the reaction was started. CAD is an internal Teflon-sealed chamber holding 5 mg of powdered catalyst. As the reaction progressed, liquid phase samples were collected at intervals of 40 min.

Organic chlorinated educts were analyzed using high-performance liquid chromatography (HPLC). The samples were shaken and equilibrated prior to injecting into the six-port valve of the solvent delivery module which consisted of acetonitrile and water (Sigma-Aldrich, HPLC grade) as solvents. These solvents were pumped in a gradient mode starting with a 95:5 ratio (acetonitrile:water) proceeding to 50:50, at the end. A C18 column (Grace Alltima), operated under reverse phase, was used for separation of compounds. Lastly, a UV–vis detector (Shimadzu, SPD-20A) with a deuterium lamp and a dual-channel mode (200/220 nm) was used to detect the compounds. A chloride selective electrode (Cole Palmer, UX-27504-08) was used for detection of HCl in the liquid samples. The fraction of Cl present in various chlorinated compounds (reactants, intermediates and products) was calculated using the following equation [32]:

$$\text{fraction of Cl in compound 'i'} = \frac{n_i(t)C_i(t)}{3(C_{TCE}(\text{time}=0)\text{-}C_{TCE}(t))}$$

where $n_i(t)$ and $C_i(t)$ are the number of chlorine atoms and concentration of compound 'i', respectively at time 't'.

2.3. Ex-situ treatment with HCl

Pristine Pd/SOMS was soaked in aqueous solution of HCl to investigate the interaction of HCl with the catalyst through a liquid medium. A catalyst amount of 0.35 g was stirred in a 400 mL aqueous solution of 0.2 M HCl in a 0.5 L three-necked flask. Prior to adding the catalyst, the flask was flushed with inert gas to remove air. The soaking experiments were performed at ambient pressure and room temperature. The concentration of HCl was chosen based on the total HCl concentration produced during the HDC reaction conducted in batch reactor if complete conversion of TCE was obtained. After soaking, the slurry was filtered, and the catalyst was washed with D.I. water to remove excess anions left on the catalyst. The filtered solid was dried overnight at 110 °C. The same experiment was repeated with a solution of 0.2 M HCl containing 10 % ethanol. All other parameters were maintained the same.

2.4. Extended X-ray absorption fine structure (EXAFS)

EXAFS experiments were performed at the insertion device beamline of the Materials and Research Collaborative Access Team (MRCAT), sector 10 of the Advanced Photon Source, Argonne National Laboratory [49]. A cryogenically cooled Si(111) monochromator with a Pt coated mirror was used for harmonics rejection. Data collection was performed in transmission mode with powder samples pressed into pellets which were supported in a holder consisting of six cylindrical holes. A hole-width of 0.12 cm^2 with an optimal catalyst amount was used to obtain a maximum edge step ($\Delta\mu x$) of 0.5 for the 1 %Pd/SOMS samples while that obtained for the Pd foil was about 1.6. Each sample spectrum was accompanied by the foil spectrum that helped in energy calibration. Data analysis was performed using WINXAS97 software following the standard procedure [50]. First derivative spectra were used to determine the threshold energy of the calibrated samples. Least square fits in R-space and k-space of the isolated nearest neighbor were used to determine EXAFS parameters such as the coordination number (CN) and interatomic bond distance (R). References such as Pd(II)chloride and Pd foil were used for obtaining phase shifts and backscattering amplitudes. For fitting purposes, CN and R associated with Pd-Cl scattering in Pd(II) chloride was 4 and 2.31 Å, respectively whereas, with Pd-Pd scattering in foil were fixed at 12 and 2.75 Å, respectively.

2.5. Near-ambient pressure X-ray photoelectron spectroscopy (NAP-XPS)

NAP-XPS experiments were performed with a lab-based SPECS system fitted with an in-situ cell and fitted with a Phoibos-HSA3500 analyzer. The system utilized an Al K-alpha source operated at 60 W and 15 kV. The powdered sample (Pd/SOMS) was loaded on carbon tapes and evacuated overnight under ultra-high vacuum conditions. Survey spectra were obtained at 100 pass energy with a dwell time of 0.1 ms and a step size of 1 eV. High resolution spectra of dry Pd/SOMS were collected with a 50 pass energy, 2.5 s dwell time at 0.1 eV steps. C1s, O1s, Pd 3d and Si 2p regions were selected for spectra collection. Ethanol (Fischer Scientific, 99.9% proof) was purified with three freeze-thaw cycles using liquid N_2 while degassing the vapor-space. An online mass spectrometer was used to confirm and monitor the composition of exit stream from the NAP-XPS cell. Initially, high resolution spectra were collected in absence of ethanol at a base pressure of lower than 5.0E-8 mbar followed by introducing ethanol at 1 mbar and raising the pressure to 3 mbar pressure. Subsequently, the chamber was evacuated, and another set of spectra were collected immediately post-evacuation to assess changes observed due to ethanol addition.

3. Results and discussion

3.1. Effect of ethanol addition on HDC of TCE

Catalytic activity experiments were performed with different concentrations of ethanol in order to investigate its role in HDC of TCE using Pd/SOMS. The results are shown in Fig. 1, wherein an increase in the concentration of ethanol (1%–10%, v/v) showed an increase in the rate of conversion of TCE. These results are consistent with those previously reported by Celik et al. [32], however, in this study, it was also found that increasing the concentration of ethanol further to 20% (v/v) led to a decrease in the rate of TCE conversion. Several studies have reported a drop in TCE conversion in presence of co-solvents such as, methanol and ethanol wherein, the enhanced solubility of TCE in the co-solvent-water mixture reduced its sorption in the catalyst [46,51]. This is consistent with our findings for concentrations of ethanol higher than 10%. For the rest of this study, ethanol concentration was fixed to be at its optimal value (10% (v/v)).

The effect of ethanol on the availability of reactants in the liquid phase is discussed in the next section.

3.1.1. Effect of ethanol on the availability of reactants

Fig. 2 shows the relationship between solubility of TCE in water-ethanol mixtures and its partition coefficient in SOMS. Partition

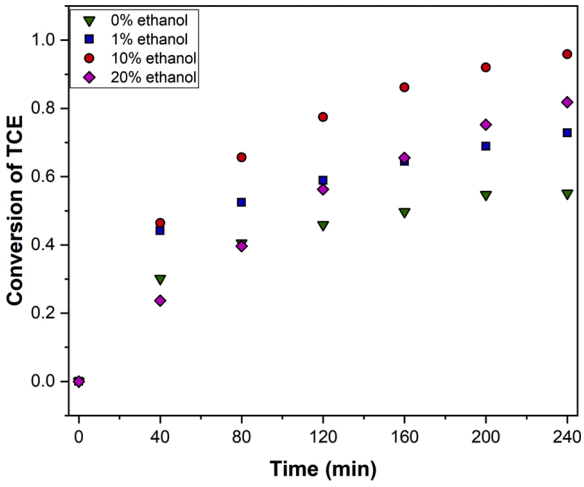

Fig. 1. Effect of concentration of ethanol on HDC of TCE using 1% Pd/SOMS; at 30 °C, 50 bar of pure H_2, 25 mg/L of catalyst.

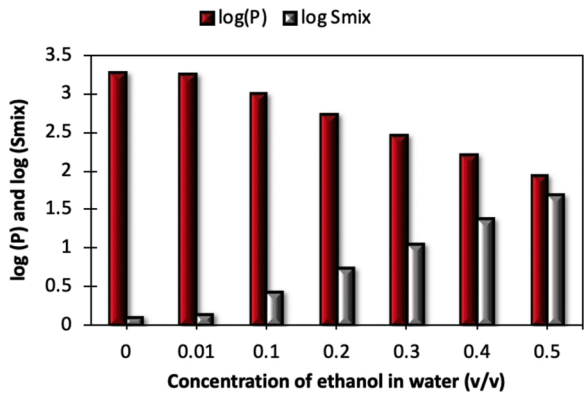

Fig. 2. Effect of ethanol content on solubility of TCE in ethanol-water mixture (Smix) and its partition coefficient (P) in SOMS.

coefficient of TCE dissolved in water-ethanol mixtures in SOMS is defined as ratio of moles of TCE bound to SOMS per mg of SOMS to concentration of TCE in the solution [3]. The log-linear model developed by Li et al. [52], along with the log-log relationship developed from results reported by Edmiston et al., was employed to calculate the partition coefficient of TCE in SOMS while dissolved in water-ethanol mixture [3,53].

According to Edmiston et. al. [3], the partition coefficient of an organic solute with respect to SOMS (P) is dependent on its octanol-water partition coefficient (K_{ow}) through a log-log relationship as follows:

$$\log P = (0.97 \times \log K_{OW}) + 0.96 \quad (1.1)$$

The octanol-water coefficient is a measure of hydrophobicity/non-polarity of the organic solute and is known to be dependent on the aqueous solubility (S_w) of that organic compound as follows [53]:

$$\log K_{OW} = -a \times \log S_W + b \quad (1.2)$$

where a, and b are constants which depend on the properties of the absorbent material.

Eq. (1.1) and (1.2) show that changes to solubility of an organic solute in the aqueous solution can cause changes to the octanol-water partition coefficient thereby altering its partition coefficient with respect to SOMS. The said changes in solubility of an organic solute in aqueous medium can be brought about by addition of another organic solvent. Thus, addition of ethanol can affect the partition coefficient of trichloroethylene (TCE) with respect to SOMS. Li et. al. developed the following log-linear relationship that allows the determination of solubility of TCE in an ethanol-water mixture (S_{mix}) using its solubility in pure water and K_{ow} values at room temperature [52]:

$$\log\left(\frac{S_{mix}}{S_w}\right) = (1.274 + 0.791 \times K_{OW}) \times f_{ethanol} \quad (1.3)$$

$f_{ethanol}$ = *volume fraction of ethanol*

Thus, a log-log relationship similar to that shown in Eq. (1.2) was determined from results reported by Edmiston et. al. [3]:

$$\log P = (-0.852 \times \log S_{mix}) + 3.37 \quad (1.4)$$

Using Eq. (1.3) and Eq. (1.4), partition coefficient of TCE with respect to SOMS was determined as a function of increasing ethanol concentration in the solution and is plotted in Fig. 2. It can be seen that high ethanol content in water suppresses the partitioning of TCE in SOMS. Addition of ethanol to the reaction mixture changes the chemical activity coefficient of TCE in the solution, thereby increasing its solubility [52,53]. Typically, these changes are more prominent above co-solvent (ethanol) concentrations of 10% (v/v) [53].

Along with TCE, the effect of ethanol on the concentration of dissolved hydrogen needs to be addressed. Due to the thermodynamically non-ideal conditions present in the liquid-phase system, rates are usually determined by the activity of the reactant gases rather than pressure. The activity of a gaseous component in a solvent is given by its solubility at that temperature and pressure [54]. Thus, the solubility of hydrogen, as affected by ethanol, was determined at a pressure of 50 bar using the correlation obtained by Purwanto et al. with <10% error [55]. These results are shown in Fig. 3 wherein, increasing the concentration of ethanol in the reaction mixture increases the concentration of dissolved hydrogen. However, it is important to elucidate the effect of the dissolved hydrogen concentration on the rate of TCE conversion in order to ensure its availability in excess. Activity experiments were performed with varied pressure of pure hydrogen in the presence and absence of ethanol. The results shown in Fig. 4 indicate that the rate of TCE conversion is not affected by the operating pressure of hydrogen from 20 bar to 50 bar. The differences observed in TCE conversions for 20 bar and 50 bar H_2 pressures are within experimental error (less than ± 10%). This implies that even if hydrogen is consumed in the reaction (as shown by TCE conversion), its replenishment from the gas phase is fast enough to maintain its quantity in excess, in the liquid phase.

3.1.2. *Mass transfer limitations*

Catalytic performance at different speeds (1400 and 2000 rpm) was found to be the same, indicating the absence of external mass transfer limitations [56,57]. The reactor was therefore operated at a speed of 2000 rpm during all runs. The Weis-Prater criterion was used to assess the presence of internal mass transfer limitations. According to this criterion, in the absence of internal mass transfer limitations, the rate of reaction does not depend on the particle size of the catalyst [58]. Therefore, the effect of particle size of SOMS on catalytic performance was investigated and, the results are presented in Fig. 5.

In the absence of ethanol, both catalysts showed similar conversion at 40 min, however the conversion at longer reaction times was higher with smaller particles. A possible explanation for this observation is that, although mass transfer limitations in the larger particles may not affect the transfer of the reactant (TCE) due to the high affinity of SOMS for organics, these limitations may affect the diffusion of the product (HCl) out of the pores. Also, this effect would be more pronounced at longer reaction times since the concentration of HCl would increase as the conversion increases. Hydrophobicity of SOMS can be responsible for slower diffusion of HCl from the pores. Yuan et al. had a similar assertion and suggested that, for a hydrophobic Pd/C catalyst, the slow HCl transport could lead to stronger inhibition of the HDC reaction performed in the liquid phase [39]. Mass transfer limitations can therefore be more prevalent in the latter part of the batch reactor run due to higher HCl concentration leading to higher inhibition. This aspect is further elaborated on in later sections. It should be noted that, the slow outward transport of HCl may restrict the inward transport of TCE. Therefore, the

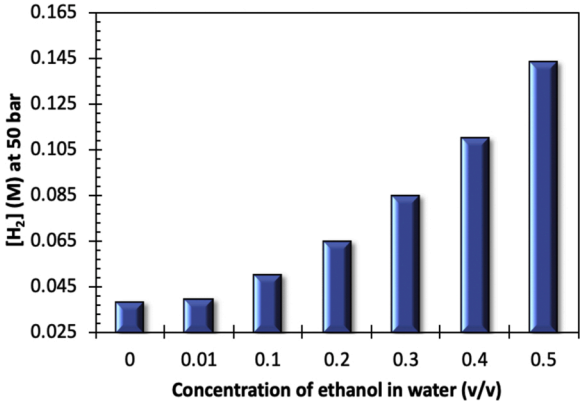

Fig. 3. Effect of ethanol content on concentration of H_2 dissolved in ethanol-water mixture at room temperature.

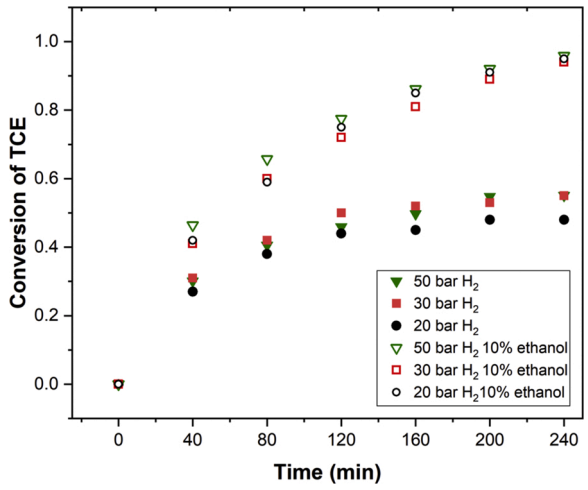

Fig. 4. Effect of pressure of H_2 on HDC of TCE using 1% Pd/SOMS; at 30 °C, 25 mg/L of catalyst.

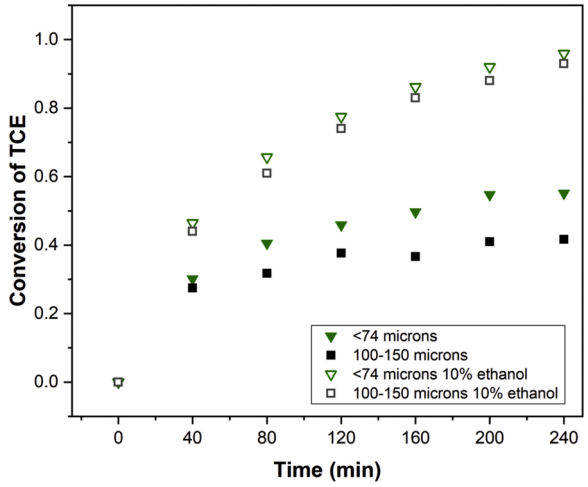

Fig. 5. Effect of particle size of SOMS on HDC of TCE using 1% Pd/SOMS; at 30 °C, 50 bar H_2, 25 mg/L of catalyst.

swelling caused by TCE entering SOMS would be lowered, resulting in collapse of the pore-structure.

Fig. 5 also shows that, in the presence of 10% ethanol, particle size did not have an effect on the activity. Thus, as per the Weis-Prater criterion, internal mass transfer limitations are absent with 10% ethanol. Ethanol concentration was constant during the course of the reaction. This is consistent with the studies performed in the literature where ethanol is used as a solvent for HDC with Pd [51,59]. Sorption of ethanol in SOMS could keep the matrix swollen throughout the reaction time, thereby maintaining a constant temporal accessibility to Pd sites. Presumably, the swelling due to ethanol can also lower inhibition by facilitating the removal of HCl from pores.

3.1.3. *Effect of ethanol on reaction intermediates*

As solvents are known to affect the reaction pathway by solvating the activated complex in kinetically relevant steps, it is important to address the effect of ethanol on the intermediates produced during HDC of TCE using Pd/SOMS [54]. Pd is known to form negligible intermediates owing to its high selectivity towards ethane and HCl, in aqueous phase at room temperature [47,60]. Besides, in case of Pd/SOMS, results obtained by in-situ Raman spectroscopy performed during HDC of TCE revealed no formation of carbonaceous deposits. However, for the commercial Pd/Al_2O_3 catalyst, carbonaceous deposits were found to be present on the surface, which was attributed to its high surface acidity [61]. During the synthesis of SOMS, the surface silanol groups (Si—OH), which could have been a potential source of any surface acidity, were capped using hexamethyldisilazane, leading to the formation of Si-O-Si $(CH_3)_3$ [4,61]. The absence of surface silanol groups was further corroborated by ^{29}Si solid-state nuclear magnetic resonance (SS-NMR) spectra, reported by Basu and Ailawar et al. [28]. Thus, it can be inferred that hydrocarbons produced as a result of HDC using Pd/SOMS do not strongly bind to the surface. However, the Pd surface could be covered with Cl species arising from partially or completely dechlorinated intermediates formed during HDC reaction.

Fig. 6 shows the Cl balance (closed up to 95%) of the HDC reaction on Pd/SOMS performed in the presence and absence of ethanol. Cl species removed from TCE appear in the partially dechlorinated compounds (DCE isomers and vinyl chloride) and HCl formed during the reaction. The fraction of Cl in each of the species in the reaction medium was calculated using the formula mentioned in Section 2.2. It is evident that the maximum fraction of Cl is present in the form of HCl (>95 %). Although, the absence (Fig. 6a) and the presence of ethanol (Fig. 6b) show marked differences in the consumption of intermediates, cis-dichloroethylene was the major intermediate in both cases. This observation is consistent with that of Lowry et al., who also reported a similar product distribution during liquid phase HDC of TCE [62]. The addition of ethanol causes further conversion of intermediates which otherwise accumulate, probably due to strong competitive adsorption of Cl species on Pd surface. This suggests that inhibitory effects caused due to strong adsorption of HCl on Pd surface could be abated by the presence of ethanol, allowing further conversion of TCE as well as intermediates on the catalyst surface. The above rationale is consistent with the that proposed by Celik et al. [32].

Due to the absence of surface-charge on SOMS ($Si-CH_3$ groups), Pd particles can be bound to the surface by non-specific interactions as

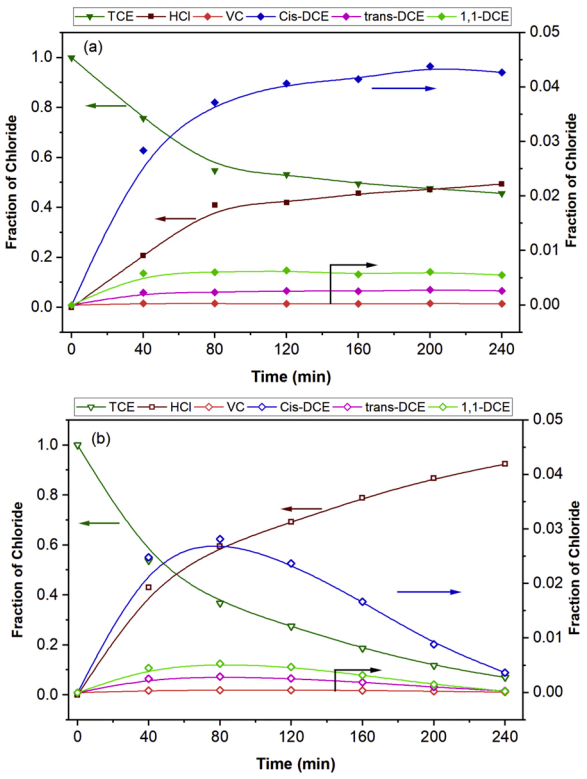

Fig. 6. Intermediates formed during HDC of TCE using 1% Pd/SOMS; at 30 °C, 50 bar H_2, 25 mg/L of catalyst performed in a) the absence of ethanol, b) the presence of 10% ethanol; TCE: trichloroethylene; VC: vinyl chloride; DCE: dichloroethylene.

opposed to strong electrostatic interactions and/or chemical interactions [61]. Hence, to address whether ethanol can leach Pd particles from SOMS matrix, Pd/SOMS was washed several times with ethanol after the synthesis. The filtrate obtained was tested with inductive plasma optical emission spectrometry (ICP-OES) which showed that no Pd leaching occurred during washing with ethanol. This indicates that ethanol is highly unlikely to cause any leaching of the Pd active sites.

3.1.4. Kinetics of HDC of TCE in the presence of ethanol

As mentioned above, the similarity in product distribution, with and without ethanol, suggests that ethanol does not affect the pathway for the HDC reaction. There are two pathways suggested for HDC of TCE in the literature, namely, sequential pathway and direct pathway. According to the sequential pathway, during HDC, an adsorbed TCE molecule undergoes H addition accompanied by Cl removal resulting in production of partially chlorinated ethenes such as dichloroethylenes (cis-DCE, trans-DCE, 1,1-DCE) and vinyl chloride which eventually get converted to ethane. Thus, Cl removal and H addition occur simultaneously for the sequential pathway. On the other hand, according to the direct pathway, an adsorbed TCE molecule loses all its chlorine atoms without any H addition. Thus, for the direct pathway, H addition is considered to occur after dechlorination resulting in the formation of ethane/ethylene [62–65]. Since, the direct pathway primarily favors complete dechlorination on the surface prior to H addition, the concentration of partially dechlorinated ethylenes (DCEs and VC) is expected to be negligible. Therefore, the occurrence of low concentration of partially dechlorinated intermediates, has prompted several researchers to conclude that HDC of TCE occurs via the direct pathway [62,65].

Besides product distribution, spectroscopic evidence in the literature also suggests the occurrence of the direct pathway. To that end, studies utilizing in-situ surface enhanced Raman spectroscopy and NMR spectroscopy have shown that polychlorinated ethylenes are likely to undergo rapid dechlorination upon adsorption on Pd, prior to H addition [60,66]. These dechlorinated surface species form radical-like intermediates which later interact with surface hydrogen producing ethane and HCl. Recently, theoretical studies using density-functional theory (DFT) and kinetic Monte Carlo simulations have also shown direct pathway to be the most probable pathway for HDC of TCE [63, 67].

Based on the direct pathway, a mechanism is proposed for HDC of TCE in the presence of ethanol, using Pd/SOMS (presented in section S1). The assumptions and derivation of the rate expression are provided in section S1. In this derivation, H_2 concentration in the reaction medium is considered to be constant, since it is replenished from the gas phase continuously. Also, the absence of internal and external mass transfer limitations with ethanol allows a kinetic analysis of the data obtained from batch-studies. In this case, kinetic analysis (linearized plots of conversion vs time shown in Fig. 7) showed that the rate appears to be first order in TCE and zero order in H_2 (refer Section 3.1.1), in presence of ethanol. This first order kinetics has been frequently encountered in the literature (refer Table S1) [62,65,68–72] and, indicates the absence of chloride inhibition.

Concerning the chloride inhibition, it should be noted that, the primary source of Cl on the Pd surface is adsorbed TCE molecules, i.e., upon adsorption, the TCE molecule is considered to undergo rapid dechlorination resulting in the formation of Pd-Cl species [60,63,67]. Thus, higher the extent of TCE dechlorination, higher is the extent of Pd chlorination. Therefore, the $[TCE]_0$/Pd ratio is important while examining aspects associated with chloride inhibition. To that end, several batch studies reported pseudo-first order behavior (no inhibition) while dealing with low initial TCE concentrations (1−10 ppm) per mg of Pd [62,65,68–72]. However, several other studies have shown that at higher initial concentration of TCE (20−100 ppm), competitive adsorption between TCE and H_2 may cause the observed order for TCE to

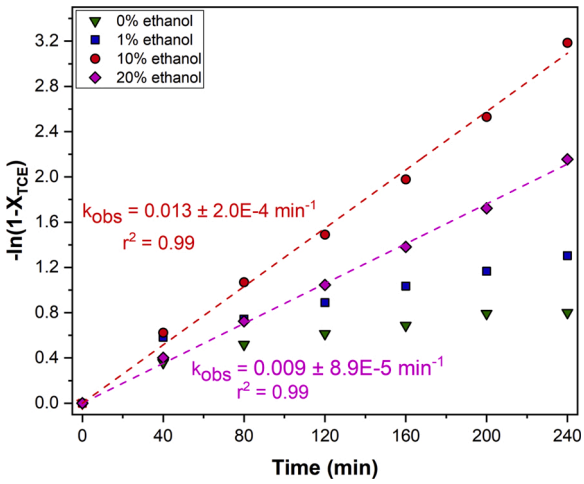

Fig. 7. -ln(1-X_{TCE}) vs time plots for HDC of TCE using 1% Pd/SOMS; at 30 °C, 50 bar H_2, 25 mg/L of catalyst with different concentrations of ethanol where X_{TCE} is the fractional conversion of TCE.

deviate from one [72–74]. With further higher concentrations of TCE (900 ppm), addition of a base/proton-scavenger is essential for the reaction to proceed with minimum deactivation at room temperature [72]. The operating conditions used in this study are more aggressive than those mentioned above (refer Table S1), yet pseudo-first order behavior with ethanol concentrations above 10% was observed indicating negligible inhibition due to HCl.

In order to reconcile this aspect, H_2 concentration relative to that of HCl must be considered. As per the proposed mechanism (Section S1), the surface Cl species can be removed by its reaction with adsorbed H atoms. During gas phase HDC of TCE, high temperature is crucial for the removal of surface Cl in the form of HCl, whereas in liquid phase, this removal is thermodynamically favored even at room temperature [63, 75]. Such a removal of Cl from the Pd surface is formulated through a reversible process as follows [76,77]:

$$H_2 + 2* \leftrightarrow 2H* \quad (1)$$

$$H* + Cl* \leftrightarrow HCl + 2* \quad (2)$$

The above reactions show that surface H species formed after dissociative adsorption of H_2 interacts with surface Cl species formed by C-Cl cleavage in TCE. This interaction results in the formation of HCl which is in equilibrium with the surface Cl and H species [76,77]. For Pd particles containing H and Cl adatoms, the recombinative desorption of H_2 and HCl are found to compete on the surface [78]. The rate of reaction between H and Cl adatoms to form HCl increases with an increase in $[H_2]$ present in the reaction medium. It follows, that under H_2-lean environment, adsorption of HCl is favored, resulting in inhibition [78]. Therefore, if the reaction is conducted in presence of excess H_2, deactivation of Pd can be suppressed. Thus, deactivation can be severe when Cl species is the most abundant surface species.

This assumption is valid mainly under high $[HCl]/[H_2]$ ratio (in other words, low H_2 concentration) and this ratio can be decreased by increasing the solubility or chemical activity of HCl in liquid phase (adding ethanol). SOMS being hydrophobic (non-polar), outward diffusion of HCl (polar) from collapsing pores could be decelerated in absence of ethanol, further leading to an increase in the local concentration of HCl. This may increase the $[HCl]/[H_2]$ ratio near the active sites. Consequently, Pd surface can be dominated by Cl species which may suppress the adsorption of reactants and intermediates. This is evident from distribution of chlorinated intermediates (Fig. 6a) during HDC of TCE, in absence of ethanol, wherein, the concentrations of TCE, HCl and intermediates change sluggishly. However, with addition of ethanol, the removal of HCl may continue unobstructed due to swelling,

resulting in higher local H_2/HCl concentrations. This explanation aids in the understanding of the observed pseudo-first order in presence of 10% ethanol.

It should be noted that, in Fig. 7, although first order behavior is not observed with 1% ethanol, the conversion of TCE shows a slow increase at longer reaction times indicating reduction in deactivation. This can be explained by considering that 1% ethanol may not be enough to swell SOMS entirely and exhibit a first-order behavior. Ethanol being easily soluble in water, its absorption in SOMS could be limited and hence, concentrations as high as 10% may be required for complete swelling.

Lastly, as shown in Fig. 7, the rate constant decreases with an increase in ethanol concentration from 10% to 20%. However, solubility of TCE in the liquid phase increases with an increase in concentration of ethanol (Fig. 2) thereby lowering the adsorption of TCE on the catalyst surface. This decrease in adsorption of TCE can result in slower reaction kinetics. Thus, concentration of ethanol affects the observed order and rate constant of the reaction.

3.1.5. *Extended X-ray absorption fine structure (EXAFS)*

Ex-situ EXAFS spectra were collected to determine the effect of ethanol on the adsorption of HCl on Pd/SOMS. Fig. 8 shows the Fourier transformed magnitude of k^2 weighted chi(k) (not corrected for phase-shift) of three Pd/SOMS catalysts. These samples were treated with aqueous solution of 0.2 M HCl in presence and absence of 10% ethanol. For comparing the changes occurring in the atomic environment of Pd, the spectra belonging to the pristine sample is also shown. Table 1 reports the EXAFS fitting results corresponding to the spectra mentioned in Fig. 8. The coordination numbers (CN) and bond distances (R) obtained are within the error-limits typically prescribed for EXAFS data-analysis [79].

The pristine sample showed presence of reduced Pd species with a CN of 8.5 and a Pd-Pd bond distance of 2.74 Å. Soaking this sample in aqueous solution of HCl led to bulk transformation of Pd particles as evidenced by the formation of Pd-Cl bonds. Pd-Pd CN decreased from 8.5–6.4 while a new Pd-Cl CN could be obtained at 1.6. Similar results were reported by Celik et al. wherein Pd/Al_2O_3 catalyst soaked in 0.01 M HCl showed formation of Pd-Cl bonds [31]. It is worth noting that, Celik et al., also reported that 0.01 M HCl led to almost complete chlorination of Pd/Al_2O_3 catalyst whereas, Pd/SOMS showed no Pd-Cl bonds. In the present study, twenty times higher HCl concentration than that used by Celik et al., was employed [31]. Therefore, it can be said that even with twenty times higher HCl concentration, only partial chlorination of Pd was observed when it was supported on SOMS (as opposed to Pd/Al_2O_3 which was completely chlorinated with only 0.01 M HCl) [31]. This difference in the extent of chlorination can be attributed to the hydrophobicity of SOMS which prevents the HCl dissolved in water to access Pd particles situated deep inside the pores. It can be further seen that, addition of ethanol during HCl treatment led to a decrease in the Pd-Cl CN from 1.6 to 1.1 with a concomitant rise in the Pd-Pd CN from 6.4–7.0, indicating that ethanol curbed the chlorination of Pd by HCl. It should be noted that the slightly higher Pd-Pd bond distance obtained for ethanol containing HCl soaked sample indicates the presence of Pd hydride formed due to the reducible action of ethanol [31,32,80]. Thus, it can be concluded that the degree of chlorination was lowered by the presence of ethanol in the solution.

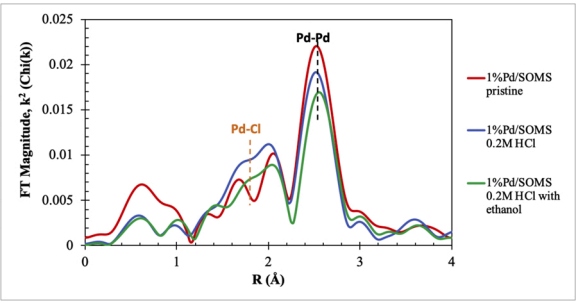

Fig. 8. Changes in the atomic environment of Pd supported on SOMS after soaking in 0.2 M HCl as well as 0.2 M HCl and 10% ethanol containing solutions.

Table 1
EXAFS fitting results showing effect of HCl on Pd/SOMS in presence and absence of ethanol.

Sample	E_o Threshold energy (eV)	Scattering Path	CN	R (Å)	$\Delta\sigma^2$ (Å^2) x10^3	E_o-shift (eV)
Pd/SOMS pristine	24350.5	Pd-Pd	8.5	2.74	3.5	−1.7
Pd/SOMS 0.2 M HCl	24352	Pd-Pd	6.4	2.75	2.6	−3.5
		Pd-Cl	1.6	2.30	4.5	−0.2
Pd/SOMS 0.2 M HCl 10% Ethanol	24352	Pd-Pd	7.0	2.78	4.2	−3.2
		Pd-Cl	1.1	2.33	4.0	0.5

These results support the assumptions made while proposing the mechanism for HDC of TCE in presence of ethanol. It was mentioned that addition of ethanol lowers the adsorption of HCl on the catalyst surface resulting in lesser deactivation. It should be noted that the presence of ethanol did not restrict the chlorination of Pd completely, yet, when added to the reaction medium complete suppression of deactivation was observed (indicated by pseudo first order behavior). This could be attributed to the presence of H_2 during the reaction which further suppresses the adsorption of HCl on Pd particles. The reversible relationship established between adsorption of H_2 and HCl further supports the conclusion that ethanol and H_2 prevent the deactivation behavior.

3.1.6. *Effect of externally added chloride species*

Besides local concentration of H_2, solution pH and surface acidity are reported to affect the HDC of TCE reaction. Acidic environment is found to promote the formation of Pd-Cl species through stabilization of the oxidized Pd by chloride ions [68,72]. Thus, chloride ions by themselves, may not be responsible for deactivation rather, low pH environment may abet inhibition [31]. In this study, addition of HCl to the reaction demonstrated the deleterious effect of HCl on the activity (Fig. 9). Owing to its low hydrophobicity, the commercial Pd/Al_2O_3 was found to deactivate. Presence of NaCl did not affect the conversion of TCE, indicating the significance of pH on catalyst deactivation (Fig. 9). In presence of chloride ions, Heck et al. employed a pH of 5.5 and reported decrease in HDC rate for Pd/Al_2O_3 [68]. However, for the same catalyst, Lowry et al. employed a pH of 9.6 and reported no change in the activity for HDC of TCE [64]. Also, our recent work investigated the difference in the activity of Pd/SOMS and Pd/Al_2O_3 treated with chloride ions, ex-situ, under different pH environments [31]. It was reported that 76% of Pd was leached from Pd/Al_2O_3 when the pH was lowered from 6.6 to 2.1. [31]. Thus, Pd/SOMS showed high deactivation resistance due to its hydrophobic nature which allowed the repulsion of these ions thereby protecting the active sites. These findings are consistent with the results reported in the current study where chloride ions were added to the reaction medium.

As mentioned previously, surface acidity may also play an important role in determining the chloride inhibition. Ordonez et al. reported that even after maintaining excess H_2 concentration, Pd/Al_2O_3 was found to deactivate [72]. Reactions performed on 5% Pd/Al_2O_3 and 5% Pd/C with similar Pd particle size (18−21 nm), under identical operating conditions, showed that the former suffered from severe deactivation [72]. This could be due to high surface acidity of Al_2O_3 promoting the inhibition due to chloride. Moreover, the reaction of HCl with Al_2O_3 may enhance its surface acidity, further abetting deactivation. As far as surface acidity of SOMS is concerned, our earlier work showed that SOMS does not possess surface acidity, which could also be responsible for its

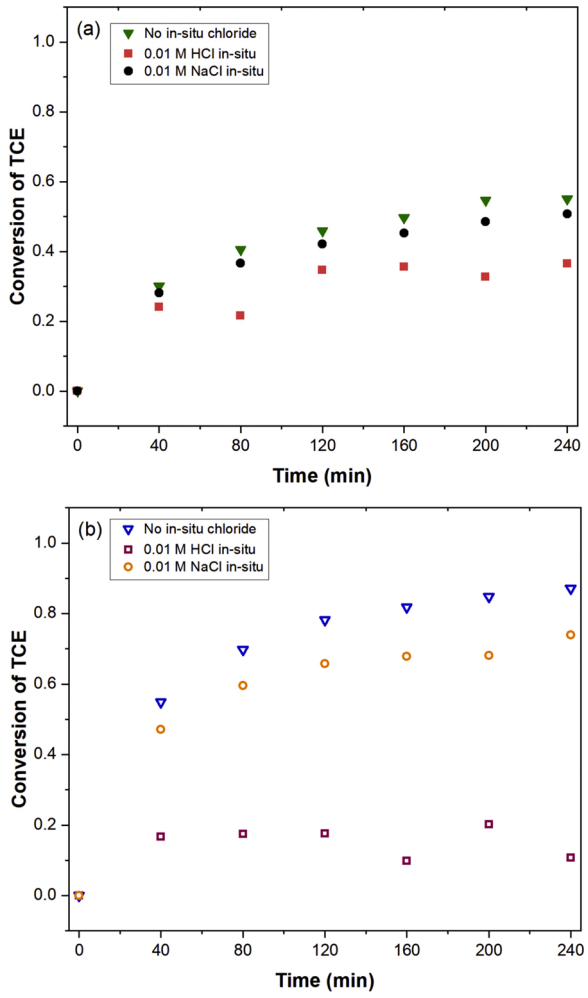

Fig. 9. Effect of externally added chloride ions on HDC of TCE using (a) 1% Pd/SOMS and (b) 1% Pd/Al_2O_3; at 30 °C, 50 bar H_2, 25 mg/L of catalyst with different pH.

better deactivation resistance [61].

3.2. Near ambient pressure X-ray photoelectron spectroscopy (NAP-XPS)

In order to further investigate the effect of concentration of ethanol, on the accessibility of Pd sites, NAP-XPS technique was used. In this case, ethanol vapors introduced into the pores of SOMS are considered to swell the catalyst through condensation in its confined porous structure. A similar behavior was previously reported by our group, using in-situ infrared spectroscopy during adsorption of vapor-phase TCE molecules [61]. In that study, the bond vibrations for adsorbed TCE molecules in SOMS, resembled those of the liquid phase molecules [61]. Studies reporting static-vapor adsorption of organics such as acetone and phenol into SOMS also support the occurrence of condensation of these molecules inside the pores to yield swollen SOMS [9,28,30].

Our previous work with NAP-XPS served as a proof of swelling of SOMS in presence of ethanol, however, the dependence of ethanol concentration on swelling was not investigated [32]. In this study, Pd/SOMS was subjected to different pressures of ethanol and the surface atomic fraction of Pd, Si, C and O species at each ethanol pressure were determined. The spectra corresponding to Pd and Si are shown in Fig. 10 and, the changes in the atomic fractions are shown in Fig. 11. and the spectra corresponding to C and O are shown in Figure S1 and, the changes in the atomic fractions are shown in Table S2.

SOMS being an insulator, significant surface charging effects were observed under UHV conditions. Due to surface charging, the peaks were found to be shifted to higher binding energies as compared to their actual positions [81,82]. The surface charging effects did not, however, lead to any peak broadening as confirmed by comparing the FWHM (full-width at half maximum) values obtained before and after ethanol introduction (see Figure S2). Therefore, the shifts in binding energies were corrected for, by using adventitious C1s as the internal standard [83,84]. Furthermore, during addition of ethanol, surface charging effects were significantly lowered, as is commonly observed for gases/-vapors introduced during AP-XPS experiments [81,84,85]. The surface charging caused by the photoelectrons was found to be neutralized by those emitted from ethanol vapors.

The surface atomic fractions are normalized with that of Si, since addition of ethanol was expected to cause changes in surface composition of O and C species and, swelling therein was expected to reveal more Pd species. The surface content of Si in this process was assumed to be constant. The signal attenuation of Pd and Si caused due to electron scattering from ethanol molecules was also considered. To that end, the total electron scattering cross section (TCS) of ethanol was found to be almost similar at higher energies (450−500 eV) which may suggest that at even higher energies the difference could be negligible [86,87]. Signal attenuation from a quasi-liquid phase of ethanol forming on the surface is also a possibility. Hence, the changes in the surface Pd/Si ratio reported here are most likely to occur due to swelling.

The results show that, as the ethanol pressure was increased, the total signal intensity for all the species was reduced. This is due to the combined effect of presence of ethanol molecules that adsorb on the surface and gas phase scattering of photoelectrons. It can be observed that the increase in ethanol pressure from 1 mbar to 3 mbar increased the Pd/Si ratio, showing that the ethanol content is directly proportional to the exposed metal species. After exposure to 3 mbar of ethanol, the environment was switched back to vacuum and spectra were collected immediately. Pd/Si ratio decreased; however, it was still higher than that prior to exposure to ethanol. Despite the fact that signal attenuation occurs from both the gas phase ethanol and ethanol molecules adsorbed onto the surface, together with the fact that photoelectrons coming from Pd 3d orbitals travel with kinetic energies slower than Si 2p orbitals (1140 eV and 1373 eV respectively) and therefore are more likely to be scattered, the ratio of Pd 3d to Si 2p continues to rise with increasing pressures of ethanol. This also confirms that with increasing concentrations of ethanol, SOMS matrix swells further and the Pd sites become more accessible to the reactant molecules.

Thus, it can be concluded that swelling of SOMS is a function of the concentration of swelling agent which further justifies the activity results reported in the previous sections.

4. Conclusion

In this study, role of ethanol in aqueous-phase HDC of TCE performed using Pd/SOMS was investigated. SOMS being a dynamic catalyst scaffold, addition of ethanol causes swelling of the matrix, influencing significant aspects such as accessibility to Pd sites and inhibition due to HCl. The absorption-induced swelling of the matrix caused by ethanol allowed the Pd sites deeply situated in the pores to be available for the reaction. This was ascertained by the Weisz-Prater criterion for investigating mass transfer limitations. Ethanol addition did not affect the product distribution; however, it altered the reaction kinetics such that the rate was observed to be pseudo-first order in TCE. Swelling of SOMS is crucial for unobstructed outward diffusion of HCl formed in the reaction, thereby increasing the ratio of H_2/HCl in the local environment of active sites. The extent of swelling, and hence, the extent of inhibition due to HCl, is directly related to the concentration of ethanol used. However, an optimal concentration of ethanol seems to exist, beyond which, rate decreased due to lower sorption of TCE on Pd sites.

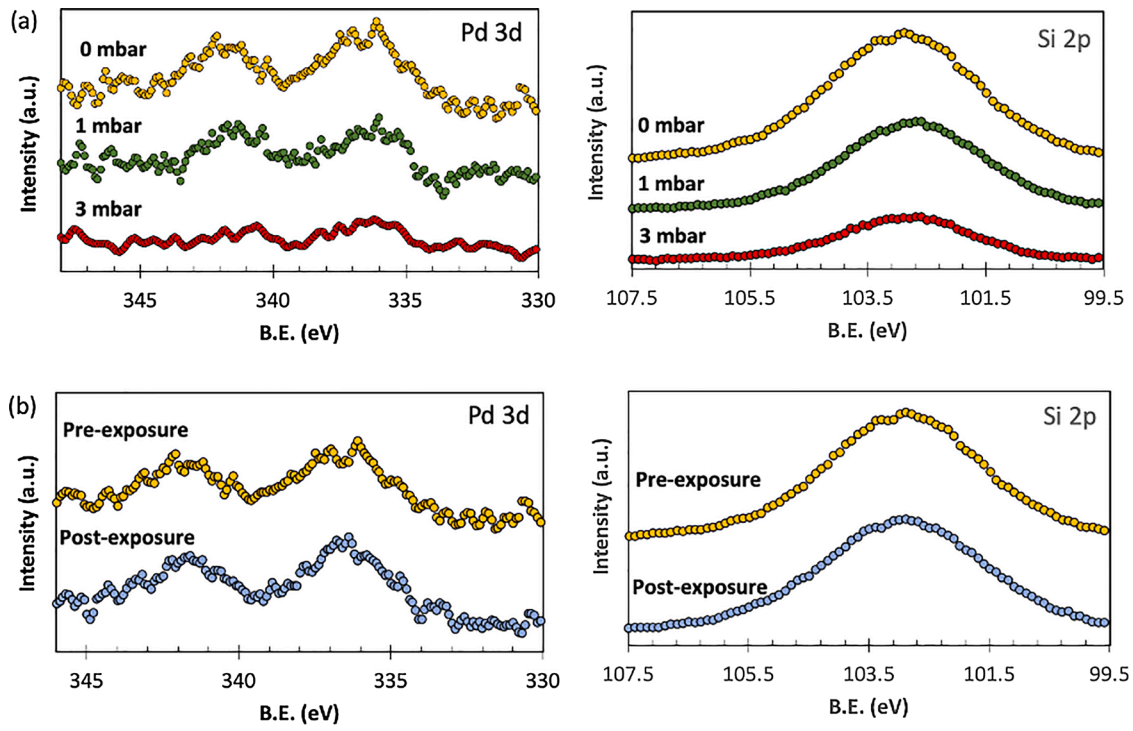

Fig. 10. NAP-XPS spectra of 1% Pd/SOMS collected at different ethanol pressures: (a) Comparison of spectra taken at 0, 1 and 3 mbar; (b) Comparison of spectra taken pre- and post-ethanol exposure.

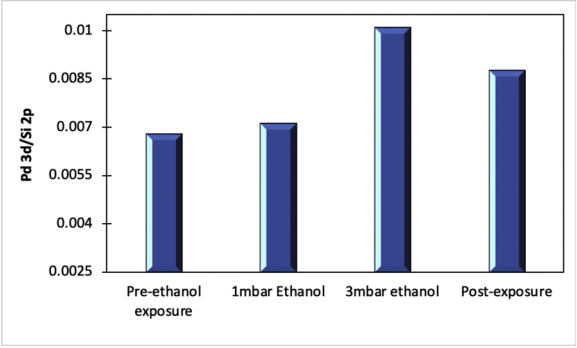

Fig. 11. Pd surface atomic fractions normalized with respect to that of Si in NAP-XPS spectra of 1% Pd/SOMS: Effect of increasing ethanol pressure.

CRediT authorship contribution statement

Saurabh Ailawar: Conceptualization, Methodology, Formal analysis, Writing - original draft, Visualization, Data curation, Investigation. **Anagha Hunoor:** Validation, Investigation, Writing - review & editing. **Yehia Khalifa:** Resources, Investigation, Writing - review & editing. **Jeffrey T. Miller:** Writing - review & editing, Funding acquisition. **Paul L. Edmiston:** Resources, Writing - review & editing. **Umit S. Ozkan:** Visualization, Writing - review & editing, Supervision, Project administration, Funding acquisition.

Declaration of Competing Interest

The authors declare that they have no known competing financial interests or personal relationships that could have appeared to influence the work reported in this paper.

Acknowledgements

This work was financially supported by the National Science Foundation through the Grant CBET- 1436729 and Ohio Coal Research Consortium. J.T.M. was supported as part of the National Science Foundation Energy Research Center for Innovative and Strategic Transformation of Alkane Resources (CISTAR) under the Cooperative Agreement No. EEC-1647722. NAP-XPS was performed at the Surface Analysis Laboratory (SAL) of the Ohio State University funded by the National Science foundation through NSF MRI award 1625792. EXAFS data was collected at the Materials Research Collaborative Access Team's (MRCAT) sector 10- ID-B at Argonne National Laboratory. MRCAT operations are supported by the Department of Energy and the MRCAT member institutions. This research used resources of the Advanced Photon Source, a U.S. Department of Energy (DOE) Office of Science User Facility operated for the DOE Office of Science by Argonne National Laboratory under Contract No. DE-AC02-06CH11357.

Appendix A. Supplementary data

Supplementary material related to this article can be found, in the online version, at doi:https://doi.org/10.1016/j.apcatb.2020.119819.

References

[1] M. Zecca, P. Centomo, B. Corain, Metal nanoclusters supported on cross-linked functional polymers: a class of emerging metal catalysts, in: B. Corain, G. Schmid, N. Toshima (Eds.), Metal Nanoclusters in Catalysis and Materials Science, 2008, pp. 201–232.

[2] C.M. Burkett, P.L. Edmiston, Highly swellable sol–gels prepared by chemical modification of silanol groups prior to drying, J. Non. Solids 351 (2005) 3174–3178.

[3] P.L. Edmiston, L.A. Underwood, Absorption of dissolved organic species from water using organically modified silica that swells, Sep. Purif. Technol. 66 (2009) 532–540.

[4] C.M. Burkett, L.A. Underwood, R.S. Volzer, J.A. Baughman, P.L. Edmiston, Organic–inorganic hybrid materials that rapidly swell in non-polar liquids: nanoscale morphology and swelling mechanism, Chem. Mater. 20 (2008) 1312–1321.

[5] U. Schubert, N. Hüsing, A. Lorenz, Hybrid inorganic-organic materials by sol-gel processing of organofunctional metal alkoxides, Chem. Mater. 7 (1995) 2010–2027.
[6] K.J. Shea, D.A. Loy, Bridged polysilsesquioxanes. Molecular-engineered hybrid organic– inorganic materials, Chem. Mater. 13 (2001) 3306–3319.
[7] K. Shea, D.A. Loy, O. Webster, Arylsilsesquioxane gels and related materials. New hybrids of organic and inorganic networks, J. Am. Chem. Soc. 114 (1992) 6700–6710.
[8] D.A. Loy, K.J. Shea, Bridged polysilsesquioxanes. Highly porous hybrid organic-inorganic materials, Chem. Rev. 95 (1995) 1431–1442.
[9] P.L. Edmiston, L.J. West, A. Chin, N. Mellor, D. Barth, Adsorption of gas phase organic compounds by swellable organically modified silica, Ind. Eng. Chem. Res. 55 (2016) 12068–12079.
[10] Z. Wang, Z. Wang, Y. Bai, B. Fu, H. Liu, A. Song, Z. Zhang, M. Zhang, Sulfonated polyethersulfone directly synthesized through sulfonic monomer as a new stable solid acid catalyst for esterification, Catal. Commun. 27 (2012) 164–168.
[11] P.A. Bonvallet, J.F. Lindner, B. Corbin, D. Crow, R. Reffner, T. Albon Riedl, S. Y. Lehman, P. Edmiston, Modeling and measuring the absorption-induced expansion of swellable organically modified silica, AIP Adv. 10 (2020) 065136.
[12] M.M. Collinson, Analytical applications of organically modified silicates, Microchim. Ichnoanal. Acta 129 (1998) 149–165.
[13] M.S. Rao, B.C. Dave, Smart" glasses: molecular programming of rapid dynamic responses in organosilica sol–gels, Adv. Mater. 14 (2002) 443–447.
[14] M.S. Rao, B.C. Dave, Thermoresponsive glasses: temperature-controlled rapid swelling and deswelling of silica-based sol–gels, Adv. Mater. 13 (2001) 274–276.
[15] L. Brannon-Peppas, N.A. Peppas, Equilibrium swelling behavior of pH-sensitive hydrogels, Chem. Eng. Sci. 46 (1991) 715–722.
[16] K. Karadag, I. Yati, H.B. Sonmez, Effective clean-up of organic liquid contaminants including BTEX, fuels, and organic solvents from the environment by poly (alkoxysilane) sorbents, J. Environ. Manage. 174 (2016) 45–54.
[17] G.O. Aydin, H.B. Sonmez, Hydrophobic poly (alkoxysilane) organogels as sorbent material for oil spill cleanup, Mar. Pollut. Bull. 96 (2015) 155–164.
[18] Y. Zhang, B. Chen, Y. Zhang, L. Qin, B. Liu, B. Ni, G. Gao, Water-enriched poly (ionic liquid) s: highly-efficient microreactors for the hydrolysis of ethylene carbonate, Green Chem. 20 (2018) 1594–1601.
[19] Y. Zhang, Y. Zhang, B. Chen, L. Qin, G. Gao, Swelling poly (Ionic liquid) s: heterogeneous catalysts that are superior than homogeneous catalyst for ethylene carbonate transformation, ChemistrySelect 2 (2017) 9443–9449.
[20] M. Wójcik-Bania, A. Krowiak, J. Strzezik, M. Hasik, Pt supported on cross-linked poly (vinylsiloxanes) and SiCO ceramics—new materials for catalytic applications, Mater. Des. 96 (2016) 171–179.
[21] S.-M. Huang, B.-L. He, One-step preparation of polymer-supported colloidal palladium catalysts and their catalytic properties II. Stability and catalytic properties in olefin hydrogenation, React. Polym. 23 (1994) 11–18.
[22] Y. Uozumi, R. Nakao, Catalytic oxidation of alcohols in water under atmospheric oxygen by use of an amphiphilic resin-dispersion of a nanopalladium catalyst, Angew. Chemie Int. Ed. 42 (2003) 194–197.
[23] M. Zecca, M. Kralik, M. Boaro, G. Palma, S. Lora, M. Zancato, B. Corain, Metal palladium supported on amphiphilic microporous synthetic organic supports. Part I. Material preparation and textural characterization, J. Mol. Catal. A Chem. 129 (1998) 27–34.
[24] R. Nakao, H. Rhee, Y. Uozumi, Hydrogenation and dehalogenation under aqueous conditions with an amphiphilic-polymer-supported nanopalladium catalyst, Org. Lett. 7 (2005) 163–165.
[25] A. Biffis, B. Corain, M. Zecca, C. Corvaja, K. Jerabek, On the macromolecular structure and molecular accessibility of swollen microporous resins: a combined ESR-ISEC approach, J. Am. Chem. Soc. 117 (1995) 1603–1606.
[26] B. Corain, M. Zecca, K. Jeràbek, Catalysis and polymer networks: the role of morphology and molecular accessibility, J. Mol. Catal. A Chem. 177 (2001) 3–20.
[27] A.A. D'Archivi, L. Galantini, A. Panatta, E. Tettamanti, B. Corain, The issue of morphology and molecular accessibility of swollen gel-type resins: an integrated inverse steric exclusion chromatography– Electron spin resonance– NMR approach, J. Phys. Chem. B 102 (1998) 6774–6779.
[28] D. Basu, S. Ailawar, G. Celik, P. Edmiston, U.S. Ozkan, Effect of high temperature on swellable organically modified silica (SOMS) and its application for preferential CO oxidation in H2 rich environment, ChemCatChem (2020) n/a.
[29] H. Sohn, G. Celik, S. Gunduz, S.S. Majumdar, S.L. Dean, P.L. Edmiston, U.S. Ozkan, Effect of high-temperature on the swellable organically-modified silica (SOMS) and its application to gas-phase hydrodechlorination of trichloroethylene, Appl. Catal. B 209 (2017) 80–90.
[30] H. Sohn, G. Celik, S. Gunduz, S.L. Dean, E. Painting, P.L. Edmiston, U.S. Ozkan, Hydrodechlorination of trichloroethylene over Pd supported on swellable organically-modified silica (SOMS), Appl. Catal. B 203 (2017) 641–653.
[31] G. Celik, S.A. Ailawar, S. Gunduz, J.T. Miller, P.L. Edmiston, U.S. Ozkan, Aqueous-phase hydrodechlorination of trichloroethylene over Pd-based swellable organically-modified silica (SOMS): Catalyst deactivation due to chloride anions, Appl. Catal. B 239 (2018) 654–664.
[32] G. Celik, S. Ailawar, H. Sohn, Y. Tang, F. Tao, J.T. Miller, P.L. Edmiston, U. S. Ozkan, Swellable organically-modified silica (SOMS) as a catalyst scaffold for catalytic treatment of water contaminated with trichloroethylene, ACS Catal. (2018).
[33] G. Celik, S.A. Ailawar, S. Gunduz, J.T. Miller, P.L. Edmiston, U.S. Ozkan, Aqueous-phase hydrodechlorination of trichloroethylene over Pd-Based swellable organically modified silica: catalyst deactivation due to sulfur species, Ind. Eng. Chem. Res. 58 (2019) 4054–4064.
[34] M.J. Moran, Occurrence and Implications of Selected Chlorinated Solvents in Ground Water and Source Water in the United States and in Drinking Water in 12 Northeast and Mid-atlantic States, 1993-2002, 2006.
[35] P.J. Squillace, C.V. Price, Urban land-use study plan for the national water-quality assessment program. US Geological Survey; Branch of Information Services [distributor], 1996.
[36] U. EPA, National Primary Drinking Water Regulations, Arsenic and Clarifications to, 2009.
[37] C.G. Schreier, M. Reinhard, Catalytic hydrodehalogenation of chlorinated ethylenes using palladium and hydrogen for the treatment of contaminated water, Chemosphere 31 (1995) 13.
[38] E. Lopez, S. Ordonez, F. Diez, Deactivation of a Pd/Al2O3 catalyst used in hydrodechlorination reactions: influence of the nature of organochlorinated compound and hydrogen chloride, Appl. Catal. B 62 (2006) 57–65.
[39] G. Yuan, M.A. Keane, Liquid phase hydrodechlorination of chlorophenols over Pd/C and Pd/Al2O3: a consideration of HCl/catalyst interactions and solution pH effects, Appl. Catal. B 52 (2004) 301–314.
[40] G. Yuan, M.A. Keane, Role of base addition in the liquid-phase hydrodechlorination of 2, 4-dichlorophenol over Pd/Al2O3 and Pd/C, J. Catal. 225 (2004) 510–522.
[41] M.I. Cobo, J.A. Conesa, C. Montes de Correa, The Effect of NaOH on the liquid-phase hydrodechlorination of dioxins over Pd/γ-Al2O3, J. Phys. Chem. A 112 (2008) 8715–8722.
[42] M.O. Nutt, J.B. Hughes, M.S. Wong, Designing Pd-on-Au bimetallic nanoparticle catalysts for trichloroethene hydrodechlorination, Environ. Sci. Technol. 39 (2005) 8.
[43] M.O. Nutt, K.N. Heck, P. Alvarez, M.S. Wong, Improved Pd-on-Au bimetallic nanoparticle catalysts for aqueous-phase trichloroethene hydrodechlorination, Appl. Catal. B 69 (2006) 115–125.
[44] B. Schrick, J.L. Blough, A.D. Jones, T.E. Mallouk, Hydrodechlorination of trichloroethylene to hydrocarbons using bimetallic nickel– iron nanoparticles, Chem. Mater. 14 (2002) 5140–5147.
[45] R. Navon, S. Eldad, K. Mackenzie, F.-D. Kopinke, Protection of palladium catalysts for hydrodechlorination of chlorinated organic compounds in wastewaters, Appl. Catal. B 119-120 (2012) 241–247.
[46] F.-D. Kopinke, D. Angeles-Wedler, D. Fritsch, K. Mackenzie, Pd-catalyzed hydrodechlorination of chlorinated aromatics in contaminated waters—effects of surfactants, organic matter and catalyst protection by silicone coating, Appl. Catal. B 96 (2010) 323–328.
[47] C. Schüth, N.-A. Kummer, C. Weidenthaler, H. Schad, Field application of a tailored catalyst for hydrodechlorinating chlorinated hydrocarbon contaminants in groundwater, Appl. Catal. B 52 (2004) 197–203.
[48] C. Schüth, S. Disser, F. Schüth, M. Reinhard, Tailoring catalysts for hydrodechlorinating chlorinated hydrocarbon contaminants in groundwater, Appl. Catal. B 28 (2000) 147–152.
[49] C. Segre, N. Leyarovska, L. Chapman, W. Lavender, P. Plag, A. King, A. Kropf, B. Bunker, K. Kemner, P. Dutta, The MRCAT insertion device beamline at the advanced photon source, in: AIP conference proceedings, Am. Inst. Phys. (2000) 419–422.
[50] T. Ressler, WinXAS: a new software package not only for the analysis of energy-dispersive XAS data, Le J. de Physique IV 7 (1997). C2-269-C262-270.
[51] H.-Y. Wee, J.A. Cunningham, Palladium-catalyzed hydrodehalogenation of 1,2,4,5-tetrachlorobenzene in water–ethanol mixtures, J. Hazard. Mater. 155 (2008) 1–9.
[52] A. Li, S.H. Yalkowsky, Solubility of organic solutes in ethanol/water mixtures, J. Pharm. Sci. 83 (1994) 1735–1740.
[53] R.P. Schwarzenbach, P.M. Gschwend, D.M. Imboden, Organic liquid water partitioning. Environmental Organic Chemistry, John Wiley & Sons, Hoboken, N.J, 2003.
[54] R.J. Madon, E. Iglesia, Catalytic reaction rates in thermodynamically non-ideal systems, J. Mol. Catal. A Chem. 163 (2000) 189–204.
[55] Purwanto, R. Deshpande, R. Chaudhari, H. Delmas, Solubility of hydrogen, carbon monoxide, and 1-octene in various solvents and solvent mixtures, J. Chem. Eng. Data 41 (1996) 1414–1417.
[56] L.K. Doraiswamy, D. Uner, Chemical reaction engineering: beyond the fundamentals, CRC press (2013).
[57] O. Levenspiel, Chemical reaction engineering, Ind. Eng. Chem. Res. 38 (1999) 4140–4143.
[58] H.S. Fogler, Elements of Chemical Reaction Engineering, 1999.
[59] J.B. Hoke, G.A. Gramiccioni, E.N. Balko, Catalytic hydrodechlorination of chlorophenols, Appl. Catal. B 1 (1992) 285–296.
[60] W. Sriwatanapongse, M. Reinhard, C.A. Klug, Reductive hydrodechlorination of trichloroethylene by palladium-on-alumina catalyst: 13C solid-state NMR study of surface reaction precursors, Langmuir 22 (2006) 4158–4164.
[61] G. Celik, S.A. Ailawar, S. Gunduz, P.L. Edmiston, U.S. Ozkan, Formation of carbonaceous deposits on Pd-based hydrodechlorination catalysts: vibrational spectroscopy investigations over Pd/Al2O3 and Pd/SOMS, Catal. Today (2018).
[62] G.V. Lowry, M. Reinhard, Hydrodehalogenation of 1- to 3-Carbon halogenated organic compounds in water using a palladium catalyst and hydrogen gas, Environ. Sci. Technol. 33 (1999) 6.
[63] J. Andersin, P. Parkkinen, K. Honkala, Pd-catalyzed hydrodehalogenation of chlorinated olefins: theoretical insights to the reaction mechanism, J. Catal. 290 (2012) 118–125.
[64] G.V. Lowry, M. Reinhard, Pd-catalyzed TCE dechlorination in groundwater: solute effects, biological control, and oxidative catalyst regeneration, Environ. Sci. Technol. 34 (2000) 3217–3223.

[65] G.V. Lowry, M. Reinhard, Pd-catalyzed TCE dechlorination in water: effect of [H2](aq) and H2-utilizing competitive solutes on the TCE dechlorination rate and product distribution, Environ. Sci. Technol. 35 (2001) 696–702.
[66] K.N. Heck, B.G. Janesko, G.E. Scuseria, N.J. Halas, M.S. Wong, Observing metal-catalyzed chemical reactions in situ using surface-enhanced Raman spectroscopy on Pd– Au nanoshells, J. Am. Chem. Soc. 130 (2008) 16592–16600.
[67] A. Kausamo, J. Andersin, K. Honkala, Mechanism of trichloroethene hydrodehalogenation: a first-principles kinetic Monte Carlo study, J. Phys. Chem. C 118 (2014) 19759–19767.
[68] K.N. Heck, M.O. Nutt, P. Alvarez, M.S. Wong, Deactivation resistance of Pd/Au nanoparticle catalysts for water-phase hydrodechlorination, J. Catal. 267 (2009) 97–104.
[69] M. Zhang, D.B. Bacik, C.B. Roberts, D. Zhao, Catalytic hydrodechlorination of trichloroethylene in water with supported CMC-stabilized palladium nanoparticles, Water Res. 47 (2013) 3706–3715.
[70] K. Mackenzie, H. Frenzel, F.-D. Kopinke, Hydrodehalogenation of halogenated hydrocarbons in water with Pd catalysts: reaction rates and surface competition, Appl. Catal. B 63 (2006) 161–167.
[71] H. Hildebrand, K. Mackenzie, F.-D. Kopinke, Pd/Fe3O4 nano-catalysts for selective dehalogenation in wastewater treatment processes—influence of water constituents, Appl. Catal. B 91 (2009) 389–396.
[72] S. Ordóñez, B.P. Vivas, F.V. Díez, Minimization of the deactivation of palladium catalysts in the hydrodechlorination of trichloroethylene in wastewaters, Appl. Catal. B 95 (2010) 288–296.
[73] Y.-L. Fang, K.N. Heck, P.J. Alvarez, M.S. Wong, Kinetics analysis of palladium/gold nanoparticles as colloidal hydrodechlorination catalysts, ACS Catal. 1 (2011) 128–138.
[74] S. Ordóñez, F.V. Díez, H. Sastre, Catalytic hydrodechlorination of chlorinated olefins over a Pd/Al2O3 catalyst: kinetics and inhibition phenomena, Ind. Eng. Chem. Res. 41 (2002) 505–511.
[75] F.-D. Kopinke, K. Mackenzie, R. Köhler, Catalytic hydrodechlorination of groundwater contaminants in water and in the gas phase using Pd/γ-Al2O3, Appl. Catal. B 44 (2003) 15–24.
[76] C. Thompson, R. Rioux, N. Chen, F. Ribeiro, Turnover rate, reaction order, and elementary steps for the hydrodechlorination of chlorofluorocarbon compounds on palladium catalysts, J. Phys. Chem. B 104 (2000) 3067–3077.
[77] F. Ribeiro, C. Gerken, G. Somorjai, C. Kellner, G. Coulston, L. Manzer, L. Abrams, Turnover rate and kinetic mechanism for the reaction of hydrodechlorination of 1, 1-dichlorotetrafluoroethane (CF 3-CFCl 2) over a polycrystalline Pd foil, Catal. Lett. 45 (1997) 149–153.
[78] D.E. Hunka, D.C. Herman, L.I. Lopez, K.D. Lormand, D.P. Land, The adsorption and reaction of HCl on Pd(111), J. Phys. Chem. B 105 (2001) 4973–4978.
[79] J. Miller, A. Kropf, Y. Zha, J. Regalbuto, L. Delannoy, C. Louis, E. Bus, J.A. van Bokhoven, The effect of gold particle size on AuAu bond length and reactivity toward oxygen in supported catalysts, J. Catal. 240 (2006) 222–234.
[80] M.W. Tew, J.T. Miller, J.A. van Bokhoven, Particle size effect of hydride formation and surface hydrogen adsorption of nanosized palladium catalysts: L3 edge vs K edge X-ray absorption spectroscopy, J. Phys. Chem. C 113 (2009) 15140–15147.
[81] D. Starr, Z. Liu, M. Hävecker, A. Knop-Gericke, H. Bluhm, Investigation of solid/vapor interfaces using ambient pressure X-ray photoelectron spectroscopy, Chem. Soc. Rev. 42 (2013) 5833–5857.
[82] J.H. Thomas, Photon Beam Damage and Charging at Solid Surfaces, in: Beam Effects, Surface Topography, and Depth Profiling in Surface Analysis, Springer, 2002, pp. 1–37.
[83] H. Bluhm, Photoelectron spectroscopy of surfaces under humid conditions, J. Electron Spectros. Relat. Phenomena 177 (2010) 71–84.
[84] L. Trotochaud, A.R. Head, O. Karslıoğlu, L. Kyhl, H. Bluhm, Ambient pressure photoelectron spectroscopy: practical considerations and experimental frontiers, J. Phys. Condens. Matter 29 (2016) 053002.
[85] O. Karslıoğlu, H. Bluhm, Ambient-pressure X-ray photoelectron spectroscopy (APXPS), in: J. Frenken, I. Groot (Eds.), Operando Research in Heterogeneous Catalysis, Springer International Publishing, Cham, 2017, pp. 31–57.
[86] D. Silva, T. Tejo, J. Muse, D. Romero, M. Khakoo, M. Lopes, Total electron scattering cross sections for methanol and ethanol at intermediate energies, Journal of Physics B: atomic, J. Phys. B At. Mol. Opt. Phys. 43 (2009), 015201.
[87] C. Szmytkowski, P. Możejko, Recent total cross section measurements in electron scattering from molecules, Eur. Phys. J. D - At. Mol. Opt. Phys. 74 (2020) 1–19.